Supplement of Biogeosciences, 19, 2699–2727, 2022
https://doi.org/10.5194/bg-19-2699-2022-supplement

Biogeosciences Open Access EGU

Supplement of

Estimating dry biomass and plant nitrogen concentration in pre-Alpine grasslands with low-cost UAS-borne multispectral data – a comparison of sensors, algorithms, and predictor sets

Anne Schucknecht et al.

Correspondence to: Anne Schucknecht (anne.schucknecht@kit.edu)

Supplementary material – table of concentration

Supplementary Tables

Table ST1. Used vegetation indices …….. 2
Table ST2. Calibrated hyper-parameters for DM and N concentration estimation ……..……...… 3
Table ST3. Overview about model quality parameters ……..…… 4
Table ST4. Mean variable importance ……..…… 6

Supplementary Figures

Figure SF1. Reflectance values for different bands and NDVI values of REM vs. SEQ sensor ……..……8
Figure SF2. Changes of best error in parameter calibration ……. 9
Figure SF3. Parameter convergence diagnosis by normalized distance ……...……...10
Figure SF4. Comparison of model quality parameters between REM and SEQ data …….……11
Figure SF5. Comparison of model quality parameters between the ML algorithms GBM and RF …… 11
Figure SF6. Comparison of model quality parameters between different predictor sets ……. 11
Figure SF7. Prediction plots of DM for cross-validation sites (FE + RB) with REM/SEQ Data ……... 12
Figure SF8. Prediction plots of N concentration for cross-validation sites (FE + RB) with REM/SEQ Data ….…….. 14
Figure SF9. Prediction plots of DM for validation site (EL) with SEQ data …….……..…… 16
Figure SF10. Prediction plots of N concentration for validation site (EL) with SEQ data ……..…..…….…... 17
Figure SF11. Spatial estimations for RB-South site ……..…..…….…….. 18
Figure SF12. Spatial estimations for FE site …….……. 19
Figure SF13. Spatial estimations for EL-North site ……..……..……..…. 20
Figure SF14. Spatial estimations for EL-South site ……..…….. 21

References of supplementary material …….. 22

Table ST1. Used vegetation indices. Ratio, orthogonal, hybrid, red edge, and modified chlorophyll indices were selected from overview of Asam (2014) and other VI from summary of Ollinger (2011). BLUE, GREEN, RED, RE, NIR = reflectance value of blue, green, red, red-edge and near-infrared band. If the reference stated a specific wavelength in their formula, we attributed the corresponding broad band (blue, green, red, red-edge, NIR) to it.

Abbreviation	Name	Formula	Reference
Ratio indices			
SR	Simple Ratio	NIR / RED	Jordan, 1969; Pearson et al., 1972
NDVI	Normalized Difference Vegetation Index	(NIR - RED) / (NIR + RED)	Rouse et al., 1974
RDVI	Renormalized Difference Vegetation Index	(NIR - RED) / (sqrt(NIR + RED))	Roujean and Breon, 1995
ARVI	Atmospherically Resistant Vegetation Index	(NIR - (RED - (BLUE - RED))) / (NIR + (RED - (BLUE - RED)))	Kaufman and Tanre, 1992
MSR1	Modified Simple Ratio 1	(NIR / RED - 1) / (sqrt(NIR / RED + 1))	Chen, 1996
MSR2	Modified Simple Ratio 2	(NIR - BLUE) / (RED - BLUE)	Sims and Gamon, 2002
Orthogonal indices			
DVI	Difference Vegetation Index	NIR - RED	Jordan, 1969
Hybrid indices			
SAVI	Soil Adjusted Vegetation Index	((1 + L) * (NIR - RED)) / (NIR + RED + L); L = 0.5	Huete, 1988
OSAVI	Optimised Soil Adjusted Vegetation Index	(1 + 0.16) * ((NIR - RED) / (NIR + RED + 0.16))	Rondeaux et al., 1996
MSAVI	Modified Soil Adjusted Vegetation Index	0.5 * (2 * NIR + 1 - sqrt((2*NIR + 1)^2 - 8 * (NIR - RED)))	Qi et al., 1994
SARVI	Soil and Atmosphere Resistant Vegetation Index	(1 + L) * ((NIR - (RED - (BLUE - RED))) / (NIR + (RED - (BLUE - RED)) + 0.5)); L = 0.5	Kaufman and Tanre, 1992
EVI	Enhanced Vegetation Index	2.5 * (NIR - RED) / (1 + NIR + C1 * RED - C2 * BLUE); C1 = 6, C2 = 7.5	Huete et al., 2002
Red edge indices			
MSRre	Modified Red Edge Simple Ratio	(NIR - BLUE) / (RE - BLUE)	Sims and Gamon, 2002
NDVIre	NDVI Red Edge	(NIR - RE) / (NIR + RE)	Gitelson and Merzlyak, 1994
RRI1	Red edge Ratio Index 1	NIR / RE	Ehammer et al., 2010
RRI2	Red edge Ratio Index 2	RE / RED	Ehammer et al., 2010
Modified chlorophyll indices			
MCARI	Modified Chlorophyll Absorption Ratio Index	((RE - RED) - 0.2 * (RE - GREEN)) * (RE / RED)	Daughtry et al., 2000
MCARI1	Modified Chlorophyll Absorption Ratio Index 1	1.2 * (2.5 *(NIR - RED) - 1.3 * (NIR - GREEN))	Haboudane et al., 2004
MCARI2	Modified Chlorophyll Absorption Ratio Index 2	(1.5 * (2.5 *(NIR - RED) - 1.3 * (NIR - GREEN))) / (sqrt((2 * NIR + 1)^2) - (6 * NIR - 5 * sqrt(RED)) - 0.5)	Haboudane et al., 2004
MTVI	Modified Triangular Vegetation Index	1.2 * (1.2 * (NIR - GREEN) - 2.5 * (RED - GREEN))	Haboudane et al., 2004
other VI (more dedicated to chlorophyll; originally hyperspectral indices)			
Datts	Datt's Index	(NIR - RE) / (NIR - RED)	Datt, 1999
aDVI	Adjusted Difference Vegetation Index	NIR - ((GREEN + RED)/2)	Broge and Leblanc, 2001
GNDVI	Green Normalized Difference Vegetation Index	(NIR - ((BLUE - GREEN)/2)) / (NIR + ((BLUE + GREEN)/2))	Gitelson and Merzlyak, 1997
$PSSR_c$	Pigment-specific simple ration for cartenoids	NIR / BLUE	Blackburn, 1998
$RARS_a$	Ratio analysis of reflectance spectra for chlorophyll a	RED / RE	Blackburn, 1999; Chappelle et al., 1992
SIPI	Structure-insensive pigment index	(NIR - BLUE) / (NIR - RED)	Penuelas et al., 1995

Table ST2. Calibrated hyper-parameters for DM and N concentration estimation. ML parameters calibrated using model-based Bayesian calibration in 500 iterations. The best parameter values were selected by lowest error. The unit of error of DM is g m^{-2} and of the N concentration is wt.%.

Response	ML algorithm	ML parameter	Sensor	PS1	PS2	PS3	PS4	PS5	PS6
DM	GBM	Shrinkage	REM	1.02E-02	2.71E-04	2.83E-04	4.94E-05	6.81E-02	3.58E-03
			SEQ	9.77E-05	8.90E-02	7.91E-05	1.16E-04	8.30E-05	4.27E-05
			REMwoBlue	6.50E-04	1.98E-04	1.10E-03	1.00E-04	7.03E-04	9.98E-05
		Interaction depth	REM	5	4	3	3	5	6
			SEQ	2	4	3	3	6	6
			REMwoBlue	5	5	1	4	4	2
		N_{tree}	REM	2000	25748	33785	49993	2028	2010
			SEQ	21870	12906	49985	49993	49994	43559
			REMwoBlue	12649	39810	13422	40750	33557	49992
		Lowest error (g m^{-2})	REM	51.58	54.48	51.33	52.48	45.81	43.82
			SEQ	60.99	58.37	57.98	54.38	48.49	49.90
			REMwoBlue	53.41	51.35	51.05	54.23	47.35	45.36
	RF	m_{try}	REM	5	5	9	1	3	23
			SEQ	1	13	15	1	2	14
			REMwoBlue	4	3	4	1	3	13
		Node size	REM	4	1	5	5	3	3
			SEQ	2	5	3	3	5	1
			REMwoBlue	2	3	1	5	5	5
		N_{tree}	REM	8511	500	3471	2992	1266	8648
			SEQ	6420	9048	3282	7706	7929	4878
			REMwoBlue	1244	5015	7687	9694	2827	7774
		Lowest error (g m^{-2})	REM	49.05	47.52	47.38	54.46	43.85	40.92
			SEQ	61.32	55.62	57.43	59.13	47.88	46.22
			REMwoBlue	47.09	47.65	47.37	59.12	43.42	40.34
N concentration	GBM	Shrinkage	REM	1.95E-04	3.26E-02	4.56E-04	5.86E-06	6.25E-02	7.48E-02
			SEQ	2.48E-04	2.60E-02	1.15E-02	5.39E-07	7.73E-04	6.80E-02
			REMwoBlue	1.84E-03	8.80E-05	1.90E-04	5.35E-05	8.27E-04	1.67E-04
		Interaction depth	REM	2	3	3	1	3	1
			SEQ	6	1	1	3	6	4
			REMwoBlue	3	4	5	1	3	3
		N_{tree}	REM	31385	2000	42101	2495	41388	35717
			SEQ	39916	2016	2003	9794	25239	2004
			REMwoBlue	5268	49995	34011	2034	13797	50000
		Lowest error (wt.%)	REM	0.50	0.53	0.52	0.57	0.51	0.49
			SEQ	0.48	0.48	0.46	0.62	0.47	0.47
			REMwoBlue	0.50	0.53	0.51	0.62	0.50	0.50
	RF	m_{try}	REM	1	9	9	1	2	17
			SEQ	1	17	19	1	1	18
			REMwoBlue	2	1	9	1	3	22
		Node size	REM	5	1	5	4	3	4
			SEQ	4	5	5	5	2	1
			REMwoBlue	5	5	5	4	4	5
		N_{tree}	REM	6800	5336	10000	7102	500	2738
			SEQ	10000	7268	10000	9566	8362	2026
			REMwoBlue	4563	5070	9356	3749	6097	5144
		Lowest error (wt.%)	REM	0.48	0.47	0.46	0.67	0.46	0.45
			SEQ	0.47	0.45	0.45	0.71	0.46	0.44
			REMwoBlue	0.47	0.48	0.48	0.71	0.45	0.46

Table ST3. Overview of the DM models and cross-validation evaluation metrics for all combinations of sensors (REM, SEQ), predictor sets (PS1: raw reflectance data; PS2: VI; PS3: raw reflectance data + VI; PS4: canopy height; PS5: raw reflectance data + canopy height; PS6: raw reflectance data + VI + canopy height), and ML algorithms (GBM, RF). The unit of $RMSE_{cv}$ and absolute $Bias_{cv}$ is g m^{-2} for DM and wt.% for N concentration. All metric values of single sensor-predictors-algorithm combinations are averages of the 10 iterations. $N_{obs, DM}$ = 82, $N_{obs, N}$ = 81.

DM							N concentration						
Sensor	**PS**	**Model**	**R^2_{cv}**	**$RMSE_{cv}$**	**$RRMSE_{cv}$**	**$Bias_{cv}$**	**Sensor**	**PS**	**Model**	**R^2_{cv}**	**$RMSE_{cv}$**	**$RRMSE_{cv}$**	**$Bias_{cv}$**
REM	PS1	GBM	0.47	53.92	0.16	0.34	**REM**	PS1	GBM	0.31	0.51	0.16	0.00
		RF	0.50	51.78	0.16	1.89			RF	0.38	0.49	0.15	0.01
		LM_full	0.01	90.65	0.27	0.21			LM_full	0.00	0.73	0.23	-0.01
		LM_best	0.01	90.60	0.27	0.00			LM_best	0.00	0.74	0.23	-0.01
	PS2	GBM	0.47	53.38	0.16	-0.85		PS2	GBM	0.31	0.54	0.17	-0.02
		RF	0.54	49.47	0.15	0.94			RF	0.40	0.48	0.15	-0.01
		LM_full	0.01	104.83	0.32	-0.70			LM_full	0.01	0.87	0.28	0.01
		LM_best	0.01	96.69	0.29	-1.76			LM_best	0.01	0.84	0.27	0.01
	PS3	GBM	0.49	52.65	0.16	-0.96		PS3	GBM	0.34	0.51	0.16	-0.03
		RF	0.55	49.25	0.15	0.34			RF	0.41	0.47	0.15	0.00
		LM_full	0.01	110.53	0.33	-4.78			LM_full	0.00	0.91	0.29	0.03
		LM_best	0.00	95.45	0.29	-1.28			LM_best	0.00	0.80	0.26	0.00
	PS4	GBM	0.40	53.26	0.16	-0.07		PS4	GBM	0.05	0.57	0.18	0.00
		RF	0.38	55.13	0.17	-0.09			RF	0.03	0.71	0.22	0.00
		LM_full	0.00	81.99	0.25	0.09			LM_full	0.01	0.57	0.18	0.00
		LM_best	0.00	81.99	0.25	0.09			LM_best	0.01	0.57	0.18	0.00
	PS5	GBM	0.59	47.77	0.14	2.07		PS5	GBM	0.36	0.52	0.17	-0.01
		RF	0.61	46.02	0.14	1.45			RF	0.43	0.47	0.15	0.00
		LM_full	0.00	91.83	0.28	0.22			LM_full	0.01	0.73	0.23	-0.01
		LM_best	0.00	91.76	0.28	-0.10			LM_best	0.01	0.73	0.23	-0.01
	PS6	GBM	0.63	44.63	0.13	0.10		PS6	GBM	0.36	0.52	0.16	-0.04
		RF	0.67	41.87	0.13	2.19			RF	0.43	0.46	0.15	-0.01
		LM_full	0.00	109.48	0.33	-2.64			LM_full	0.00	0.89	0.28	0.02
		LM_best	0.00	98.96	0.30	-1.68			LM_best	0.01	0.82	0.26	-0.01
SEQ	PS1	GBM	0.30	61.31	0.18	0.16	**SEQ**	PS1	GBM	0.39	0.48	0.15	0.01
		RF	0.30	61.77	0.19	-0.97			RF	0.40	0.47	0.15	0.01
		LM_full	0.00	87.51	0.26	-0.74			LM_full	0.01	0.75	0.24	0.00
		LM_best	0.00	87.77	0.26	-0.04			LM_best	0.01	0.75	0.24	0.00
	PS2	GBM	0.38	59.04	0.18	-2.48		PS2	GBM	0.38	0.50	0.16	0.00
		RF	0.40	56.69	0.17	0.10			RF	0.43	0.46	0.15	0.00
		LM_full	0.00	92.51	0.28	-0.98			LM_full	0.01	0.85	0.27	-0.01
		LM_best	0.00	90.20	0.27	-0.74			LM_best	0.00	0.79	0.25	0.01
	PS3	GBM	0.36	58.28	0.18	-0.48		PS3	GBM	0.42	0.48	0.15	0.00
		RF	0.37	58.43	0.18	-0.09			RF	0.44	0.46	0.15	0.00
		LM_full	0.01	91.25	0.27	-0.27			LM_full	0.01	0.87	0.28	-0.01
		LM_best	0.00	88.77	0.27	0.09			LM_best	0.00	0.77	0.24	0.00
	PS4	GBM	0.44	54.83	0.16	0.19		PS4	GBM	0.05	0.62	0.20	0.00
		RF	0.35	60.70	0.18	-0.06			RF	0.02	0.72	0.23	0.00
		LM_full	0.00	83.93	0.25	0.27			LM_full	0.04	0.62	0.20	0.00
		LM_best	0.00	83.93	0.25	0.27			LM_best	0.04	0.62	0.20	0.00
	PS5	GBM	0.54	49.51	0.15	0.40		PS5	GBM	0.44	0.46	0.15	0.01
		RF	0.56	48.20	0.14	-0.09			RF	0.43	0.46	0.15	0.00
		LM_full	0.00	91.03	0.27	-0.07			LM_full	0.01	0.75	0.24	0.00
		LM_best	0.00	91.08	0.27	0.24			LM_best	0.01	0.76	0.24	-0.01
	PS6	GBM	0.55	50.36	0.15	0.19		PS6	GBM	0.43	0.48	0.15	-0.01
		RF	0.56	48.39	0.15	0.07			RF	0.47	0.45	0.14	0.00
		LM_full	0.01	94.06	0.28	0.17			LM_full	0.01	0.87	0.28	-0.01
		LM_best	0.00	92.57	0.28	0.91			LM_best	0.00	0.77	0.24	0.00

Table ST3 (cont.). Overview of the DM models and cross-validation evaluation metrics for all combinations of sensors (REM, SEQ), predictor sets (PS1: raw reflectance data; PS2: VI; PS3: raw reflectance data + VI; PS4: canopy height; PS5: raw reflectance data + canopy height; PS6: raw reflectance data + VI + canopy height), and ML algorithms (GBM, RF). The unit of $RMSE_{cv}$ and absolute $bias_{cv}$ is g m^{-2} for DM and wt.% for N concentration. All metric values of single sensor-predictors-algorithm combinations are averages of the 10 iterations. $N_{obs, DM} = 82$, $N_{obs, N} = 81$.

DM							N concentration						
Sensor	**PS**	**Model**	**R^2_{cv}**	**$RMSE_{cv}$**	**$RRMSE_{cv}$**	**$Bias_{cv}$**	**Sensor**	**PS**	**Model**	**R^2_{cv}**	**$RMSE_{cv}$**	**$RRMSE_{cv}$**	**$Bias_{cv}$**
REM without blue band	PS1	GBM	0.44	54.55	0.16	0.80	**REM without blue band**	PS1	GBM	0.33	0.51	0.16	0.00
		RF	0.52	51.08	0.15	1.19			RF	0.40	0.48	0.15	0.01
		LM_full	0.01	89.96	0.27	0.11			LM_full	0.01	0.74	0.23	-0.01
		LM_best	0.01	89.67	0.27	0.28			LM_best	0.01	0.74	0.23	-0.01
	PS2	GBM	0.49	51.99	0.16	-0.65		PS2	GBM	0.24	0.54	0.17	0.00
		RF	0.55	48.89	0.15	0.57			RF	0.38	0.49	0.16	0.00
		LM_full	0.01	99.85	0.30	1.00			LM_full	0.01	0.84	0.27	0.02
		LM_best	0.01	97.00	0.29	-0.72			LM_best	0.01	0.79	0.25	0.00
	PS3	GBM	0.52	50.72	0.15	-1.31		PS3	GBM	0.31	0.51	0.16	-0.01
		RF	0.56	48.65	0.15	0.33			RF	0.38	0.49	0.15	0.00
		LM_full	0.01	101.57	0.31	0.69			LM_full	0.01	0.85	0.27	0.01
		LM_best	0.01	94.18	0.28	-1.57			LM_best	0.01	0.78	0.25	0.00
	PS4	GBM	0.44	54.87	0.16	0.20		PS4	GBM	0.08	0.62	0.20	0.00
		RF	0.35	60.26	0.18	0.19			RF	0.01	0.73	0.23	0.01
		LM_full	0.00	83.93	0.25	0.27			LM_full	0.04	0.62	0.20	0.00
		LM_best	0.00	83.93	0.25	0.27			LM_best	0.04	0.62	0.20	0.00
	PS5	GBM	0.58	47.89	0.14	0.90		PS5	GBM	0.32	0.51	0.16	-0.01
		RF	0.62	45.35	0.14	0.62			RF	0.44	0.46	0.15	0.00
		LM_full	0.00	91.36	0.27	0.35			LM_full	0.01	0.74	0.23	-0.01
		LM_best	0.00	92.21	0.28	0.28			LM_best	0.01	0.74	0.23	-0.02
	PS6	GBM	0.64	44.25	0.13	0.20		PS6	GBM	0.33	0.51	0.16	-0.01
		RF	0.68	41.35	0.12	1.52			RF	0.42	0.47	0.15	-0.01
		LM_full	0.00	101.77	0.31	2.47			LM_full	0.01	0.85	0.27	0.01
		LM_best	0.01	96.76	0.29	-2.37			LM_best	0.01	0.78	0.25	0.00

Table ST4. Mean variable importance of all parameter, sensor, predictor set and ML algorithm combinations from the 10 iterations. Unit is mean relative influence (%).

	DM								N concentration							
	REM				SEQ				REM				SEQ			
PS	**Predictor**	**GBM**	**Predictor**	**RF**	**Predictor**	**GBM**	**Predictor**	**RF**	**Predictor**	**GBM**	**Predictor**	**RF**	**Predictor**	**GBM**	**Predictor**	**RF**
PS1	R_840	0.36	R_840	0.38	R_790	0.55	R_790	0.31	R_560	0.28	R_668	0.21	R_790	0.46	R_735	0.30
	R_475	0.19	R_668	0.26	R_735	0.21	R_660	0.28	R_475	0.22	R_840	0.21	R_550	0.18	R_790	0.29
	R_717	0.18	R_717	0.14	R_550	0.12	R_735	0.27	R_840	0.21	R_475	0.21	R_735	0.18	R_660	0.25
	R_668	0.18	R_475	0.11	R_660	0.11	R_550	0.14	R_668	0.17	R_560	0.20	R_660	0.17	R_550	0.16
	R_560	0.09	R_560	0.10					R_717	0.11	R_717	0.16				
PS2	Datts	0.20	NDVIre	0.06	Datts	0.13	MCARI	0.14	MSR2	0.16	SIPI	0.06	MCARI2	0.16	RRI1	0.09
	MCARI2	0.11	RRI1	0.06	MCARI2	0.13	RARSa	0.09	MCARI2	0.14	RARSa	0.05	MCARI	0.12	NDVIre	0.09
	NDVIre	0.06	Datts	0.06	MCARI	0.11	NDVIre	0.09	SIPI	0.09	MCARI	0.05	Datts	0.10	aDVI	0.08
	RRI1	0.06	MSRre	0.05	NDVIre	0.08	RRI1	0.09	Datts	0.08	RRI1	0.05	NDVIre	0.10	DVI	0.06
	MSRre	0.05	RARSa	0.05	RRI1	0.08	Datts	0.09	MCARI	0.06	NDVIre	0.05	RRI1	0.10	RARSa	0.06
	MCARI	0.05	RRI2	0.05	RRI2	0.08	RRI2	0.07	PSSRc	0.04	MSRre	0.05	RRI2	0.07	MCARI	0.06
	MSR2	0.05	MCARI	0.04	RARSa	0.07	NDVI	0.04	MSRre	0.04	MSR2	0.05	RARSa	0.07	MSR1	0.05
	PSSRc	0.04	GNDVI	0.04	SR	0.04	SR	0.04	GNDVI	0.04	PSSRc	0.05	OSAVI	0.04	NDVI	0.05
	GNDVI	0.04	PSSRc	0.04	MSR1	0.04	MSR1	0.04	RARSa	0.04	RRI2	0.04	MSR1	0.03	SR	0.05
	aDVI	0.03	NDVI	0.04	NDVI	0.04	MSAVI	0.04	ARVI	0.04	GNDVI	0.04	NDVI	0.03	RRI2	0.05
	OSAVI	0.03	MSR1	0.04	aDVI	0.04	OSAVI	0.04	RRI2	0.04	Datts	0.04	SR	0.03	MCARI2	0.05
	MTVI	0.03	SR	0.04	DVI	0.04	DVI	0.04	RRI1	0.03	ARVI	0.03	aDVI	0.03	OSAVI	0.05
	MCARI1	0.03	ARVI	0.04	MTVI	0.03	aDVI	0.04	NDVIre	0.03	aDVI	0.03	DVI	0.03	Datts	0.05
	SIPI	0.02	OSAVI	0.04	MCARI1	0.03	SAVI	0.03	OSAVI	0.02	MSR1	0.03	MSAVI	0.02	MSAVI	0.04
	DVI	0.02	SIPI	0.03	OSAVI	0.02	MCARI1	0.03	SARVI	0.02	SR	0.03	MTVI	0.02	MCARI1	0.04
	SARVI	0.02	MCARI2	0.03	MSAVI	0.02	MTVI	0.03	MCARI1	0.01	NDVI	0.03	MCARI1	0.02	MTVI	0.04
	MSAVI	0.02	MTVI	0.03	SAVI	0.02	RDVI	0.03	MTVI	0.01	DVI	0.03	RDVI	0.02	SAVI	0.04
	EVI	0.02	MCARI1	0.03	RDVI	0.01	MCARI2	0.02	SR	0.01	MCARI1	0.03	SAVI	0.02	RDVI	0.04
	RDVI	0.01	aDVI	0.03					DVI	0.01	OSAVI	0.03				
	SAVI	0.01	SARVI	0.03					NDVI	0.01	MTVI	0.03				
	ARVI	0.01	RDVI	0.03					aDVI	0.01	EVI	0.03				
	RARSa	0.01	DVI	0.03					MSR1	0.01	MSAVI	0.03				
	RRI2	0.01	MSAVI	0.03					EVI	0.01	RDVI	0.03				
	SR	0.01	SAVI	0.03					MSAVI	0.01	SARVI	0.03				
	NDVI	0.01	EVI	0.03					SAVI	0.01	SAVI	0.03				
	MSR1	0.01	MSR2	0.02					RDVI	0.01	MCARI2	0.03				
PS3	Datts	0.18	NDVIre	0.06	Datts	0.14	MCARI	0.11	R_560	0.11	R_475	0.07	MCARI2	0.12	RRI1	0.08
	MCARI2	0.10	RRI1	0.06	R_735	0.11	RRI1	0.08	MCARI2	0.11	SIPI	0.05	RRI1	0.10	NDVIre	0.08
	NDVIre	0.06	Datts	0.06	NDVIre	0.10	NDVIre	0.08	MSR2	0.11	MCARI	0.04	NDVIre	0.10	R_735	0.07
	RRI1	0.06	RARSa	0.05	RRI1	0.10	Datts	0.08	R_475	0.08	RARSa	0.04	R_550	0.08	aDVI	0.06
	MCARI	0.05	MSRre	0.05	MCARI	0.07	RARSa	0.07	Datts	0.07	MSR2	0.04	MCARI	0.08	MCARI	0.05
	MSRre	0.05	RRI2	0.05	R_660	0.07	R_735	0.07	R_668	0.05	NDVIre	0.04	R_735	0.08	DVI	0.05
	MSR2	0.05	GNDVI	0.04	R_550	0.07	RRI2	0.06	R_717	0.05	RRI1	0.04	R_660	0.06	RARSa	0.05
	R_475	0.05	R_668	0.04	R_790	0.05	R_790	0.04	SIPI	0.05	R_668	0.04	Datts	0.05	R_790	0.05
	R_717	0.04	PSSRc	0.04	MCARI2	0.05	MSAVI	0.04	MCARI	0.04	MSRre	0.04	RARSa	0.04	R_550	0.04
	GNDVI	0.04	MCARI	0.04	RARSa	0.03	OSAVI	0.04	PSSRc	0.03	PSSRc	0.04	RRI2	0.04	RRI2	0.04
	R_840	0.04	NDVI	0.03	RRI2	0.03	SR	0.04	MSRre	0.03	RRI2	0.03	OSAVI	0.04	SR	0.04
	PSSRc	0.04	MSR1	0.03	aDVI	0.02	MSR1	0.03	GNDVI	0.03	Datts	0.03	NDVI	0.03	MSR1	0.04
	R_668	0.03	SR	0.03	DVI	0.02	NDVI	0.03	ARVI	0.02	R_560	0.03	MSR1	0.03	NDVI	0.04
	OSAVI	0.03	ARVI	0.03	MTVI	0.02	DVI	0.03	R_840	0.02	GNDVI	0.03	SR	0.03	MCARI2	0.04
	aDVI	0.02	OSAVI	0.03	MCARI1	0.02	aDVI	0.03	RRI2	0.02	R_840	0.03	R_790	0.03	OSAVI	0.04
	SARVI	0.02	SIPI	0.03	SR	0.02	SAVI	0.03	RARSa	0.02	SR	0.03	aDVI	0.02	Datts	0.04
	SIPI	0.02	R_717	0.03	NDVI	0.02	MTVI	0.03	RRI1	0.02	MSR1	0.03	MSAVI	0.02	R_660	0.04
	MCARI1	0.01	R_475	0.02	MSR1	0.02	MCARI1	0.03	NDVIre	0.02	NDVI	0.03	SAVI	0.01	MSAVI	0.03
	MTVI	0.01	MCARI2	0.02	MSAVI	0.01	RDVI	0.03	SARVI	0.01	aDVI	0.03	DVI	0.01	SAVI	0.03
	MSAVI	0.01	R_560	0.02	SAVI	0.01	MCARI2	0.02	OSAVI	0.01	ARVI	0.03	RDVI	0.01	MTVI	0.03
	DVI	0.01	MCARI1	0.02	RDVI	0.01	R_660	0.02	aDVI	0.01	DVI	0.03	MTVI	0.01	MCARI1	0.03
	EVI	0.01	MTVI	0.02	OSAVI	0.01	R_550	0.01	MCARI1	0.01	OSAVI	0.03	MCARI1	0.01	RDVI	0.03
	R_560	0.01	MSR2	0.02					MTVI	0.01	MTVI	0.02				
	ARVI	0.01	R_840	0.02					DVI	0.01	MCARI1	0.02				
	RDVI	0.01	aDVI	0.02					NDVI	0.01	EVI	0.02				
	SAVI	0.01	SARVI	0.02					SR	0.01	MSAVI	0.02				
	SR	0.01	RDVI	0.02					MSR1	0.01	SARVI	0.02				
	MSR1	0.01	EVI	0.02					EVI	0.01	RDVI	0.02				
	NDVI	0.01	DVI	0.02					MSAVI	0.01	SAVI	0.02				
	RARSa	0.01	MSAVI	0.02					SAVI	0	R_717	0.02				
	RRI2	0.01	SAVI	0.02					RDVI	0	MCARI2	0.02				

Table ST4 (continued). Mean variable importance of all parameter, sensor, predictor set and ML algorithm combinations from the 10 iterations. Unit is mean relative influence (%).

	DM								N concentration							
	REM				SEQ				REM				SEQ			
PS	**Predictor**	**GBM**	**Predictor**	**RF**	**Predictor**	**GBM**	**Predictor**	**RF**	**Predictor**	**GBM**	**Predictor**	**RF**	**Predictor**	**GBM**	**Predictor**	**RF**
PS4	CH	1.00	CH	1.00	CH	1.00	CH	1.00	CH	1.00	CH	1.00	CH	1.00	CH	1.00
PS5	CH	0.35	CH	0.30	CH	0.52	CH	0.37	R_560	0.2	R_475	0.22	R_790	0.37	R_790	0.26
	R_840	0.17	R_668	0.20	R_790	0.24	R_790	0.19	R_840	0.18	R_668	0.20	CH	0.2	R_735	0.26
	R_475	0.14	R_717	0.15	R_735	0.10	R_735	0.16	R_475	0.18	R_840	0.19	R_550	0.15	R_660	0.22
	R_668	0.13	R_840	0.15	R_550	0.08	R_550	0.15	CH	0.17	R_560	0.17	R_735	0.15	R_550	0.14
	R_717	0.13	R_475	0.11	R_660	0.07	R_660	0.14	R_668	0.15	R_717	0.12	R_660	0.14	CH	0.13
	R_560	0.09	R_560	0.10					R_717	0.12	CH	0.10				
PS6	CH	0.29	CH	0.14	CH	0.47	CH	0.2	MSR2	0.10	R_475	0.09	CH	0.12	NDVIre	0.08
	Datts	0.17	Datts	0.08	Datts	0.08	MCARI	0.07	R_560	0.10	MCARI	0.05	MCARI2	0.11	RRI1	0.08
	MCARI2	0.08	RARSa	0.06	RRI1	0.07	RARSa	0.06	MCARI2	0.10	CH	0.05	NDVIre	0.08	CH	0.08
	NDVIre	0.05	RRI1	0.05	NDVIre	0.07	RRI1	0.05	CH	0.08	SIPI	0.05	RRI1	0.08	R_735	0.06
	RRI1	0.05	NDVIre	0.05	R_735	0.05	NDVIre	0.05	R_475	0.08	MSR2	0.05	R_550	0.07	aDVI	0.06
	MSRre	0.04	RRI2	0.05	R_550	0.04	R_550	0.05	Datts	0.07	RARSa	0.04	Datts	0.07	DVI	0.05
	MSR2	0.03	MSRre	0.04	R_790	0.03	RRI2	0.05	R_717	0.05	MSRre	0.04	R_735	0.07	R_790	0.05
	MCARI	0.03	R_668	0.04	MCARI	0.02	Datts	0.05	SIPI	0.04	RRI1	0.04	MCARI	0.06	RARSa	0.04
	R_475	0.03	MCARI	0.04	R_660	0.02	R_735	0.04	MCARI	0.04	NDVIre	0.04	R_660	0.06	MCARI	0.04
	PSSRc	0.02	GNDVI	0.03	MTVI	0.02	OSAVI	0.03	R_668	0.04	R_668	0.04	RARSa	0.04	R_550	0.04
	R_717	0.02	PSSRc	0.03	MCARI1	0.02	MSAVI	0.03	MSRre	0.03	Datts	0.04	RRI2	0.04	OSAVI	0.04
	R_840	0.02	ARVI	0.03	RARSa	0.01	R_790	0.03	PSSRc	0.03	R_560	0.04	OSAVI	0.03	RRI2	0.04
	R_668	0.02	MCARI2	0.03	aDVI	0.01	MCARI1	0.03	GNDVI	0.03	PSSRc	0.03	MSR1	0.02	MCARI2	0.03
	GNDVI	0.02	SIPI	0.03	DVI	0.01	MTVI	0.03	R_840	0.02	RRI2	0.03	SR	0.02	Datts	0.03
	OSAVI	0.02	R_717	0.03	RRI2	0.01	DVI	0.03	RRI1	0.02	GNDVI	0.03	R_790	0.02	MSAVI	0.03
	SIPI	0.02	MSR1	0.02	MSAVI	0.01	aDVI	0.03	ARVI	0.02	R_840	0.03	NDVI	0.02	SAVI	0.03
	aDVI	0.01	NDVI	0.02	MCARI2	0.01	SAVI	0.03	NDVIre	0.02	ARVI	0.02	aDVI	0.02	MSR1	0.03
	ARVI	0.01	SR	0.02	OSAVI	0.01	MSR1	0.02	RRI2	0.02	NDVI	0.02	MSAVI	0.02	NDVI	0.03
	SARVI	0.01	R_475	0.02	RDVI	0.01	SR	0.02	RARSa	0.02	SR	0.02	DVI	0.01	RDVI	0.03
	R_560	0.01	R_560	0.02	SAVI	0.01	RDVI	0.02	SARVI	0.01	MSR1	0.02	MCARI1	0.01	SR	0.03
	MSAVI	0.01	MSR2	0.02	SR	0.00	NDVI	0.02	OSAVI	0.01	aDVI	0.02	SAVI	0.01	MTVI	0.03
	DVI	0.01	OSAVI	0.02	MSR1	0.00	R_660	0.02	MCARI1	0.01	DVI	0.02	MTVI	0.01	MCARI1	0.03
	EVI	0.01	SARVI	0.02	NDVI	0.00	MCARI2	0.02	DVI	0.01	MCARI2	0.02	RDVI	0.01	R_660	0.03
	MCARI1	0.01	MCARI1	0.01					MTVI	0.01	OSAVI	0.02				
	MTVI	0.01	MTVI	0.01					aDVI	0.01	MTVI	0.02				
	RRI2	0.01	MSAVI	0.01					MSR1	0.01	MCARI1	0.02				
	RARSa	0.01	RDVI	0.01					NDVI	0.01	EVI	0.02				
	RDVI	0.01	aDVI	0.01					SR	0.01	SAVI	0.02				
	NDVI	0.01	EVI	0.01					EVI	0.01	MSAVI	0.02				
	SR	0.01	SAVI	0.01					MSAVI	0.00	R_717	0.02				
	MSR1	0.00	R_840	0.01					SAVI	0.00	SARVI	0.02				
	SAVI	0.00	DVI	0.01					RDVI	0.00	RDVI	0.02				

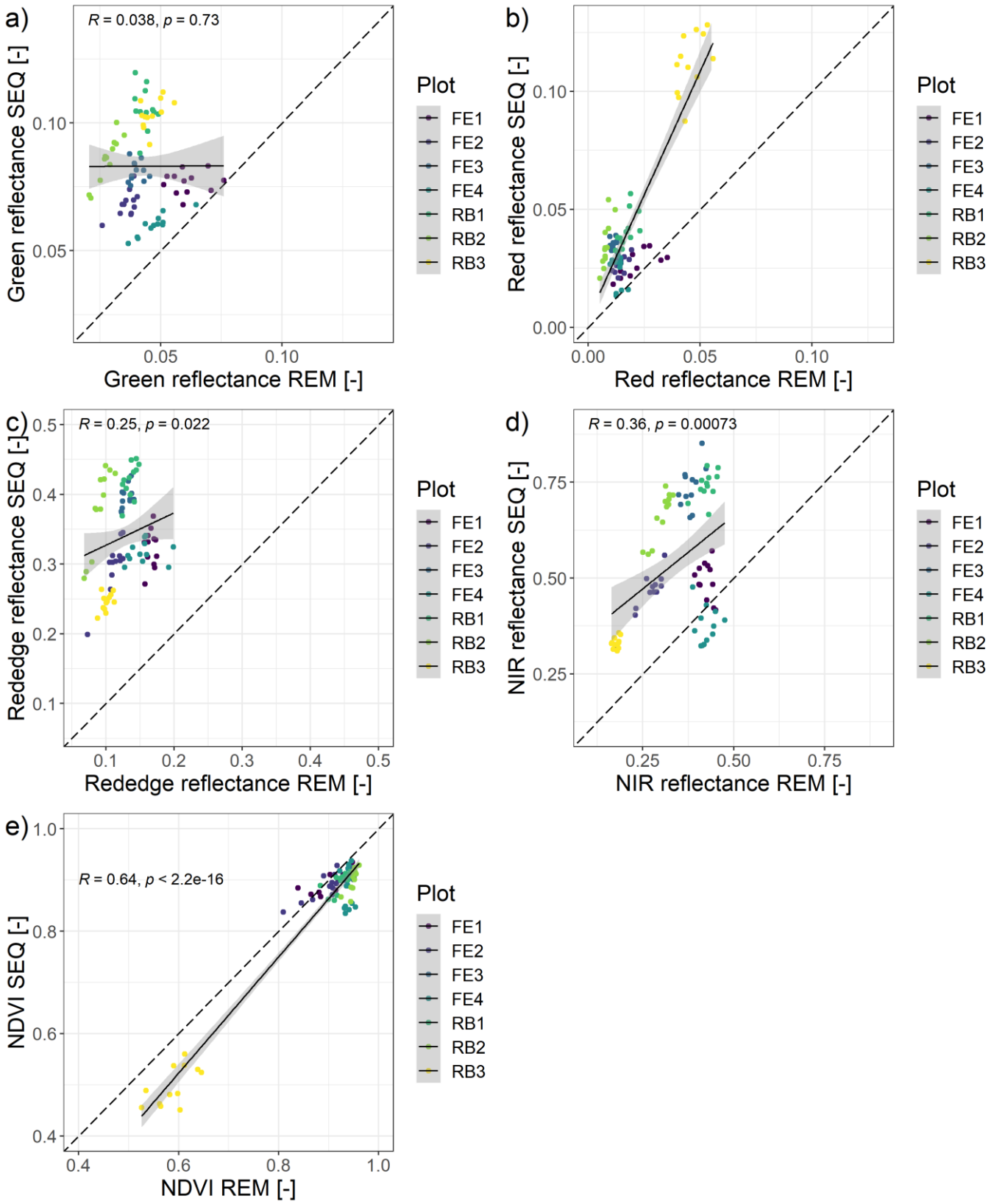

Figure SF1. Reflectance values for different bands (a-d) and NDVI values (e) of REM vs. SEQ sensor.

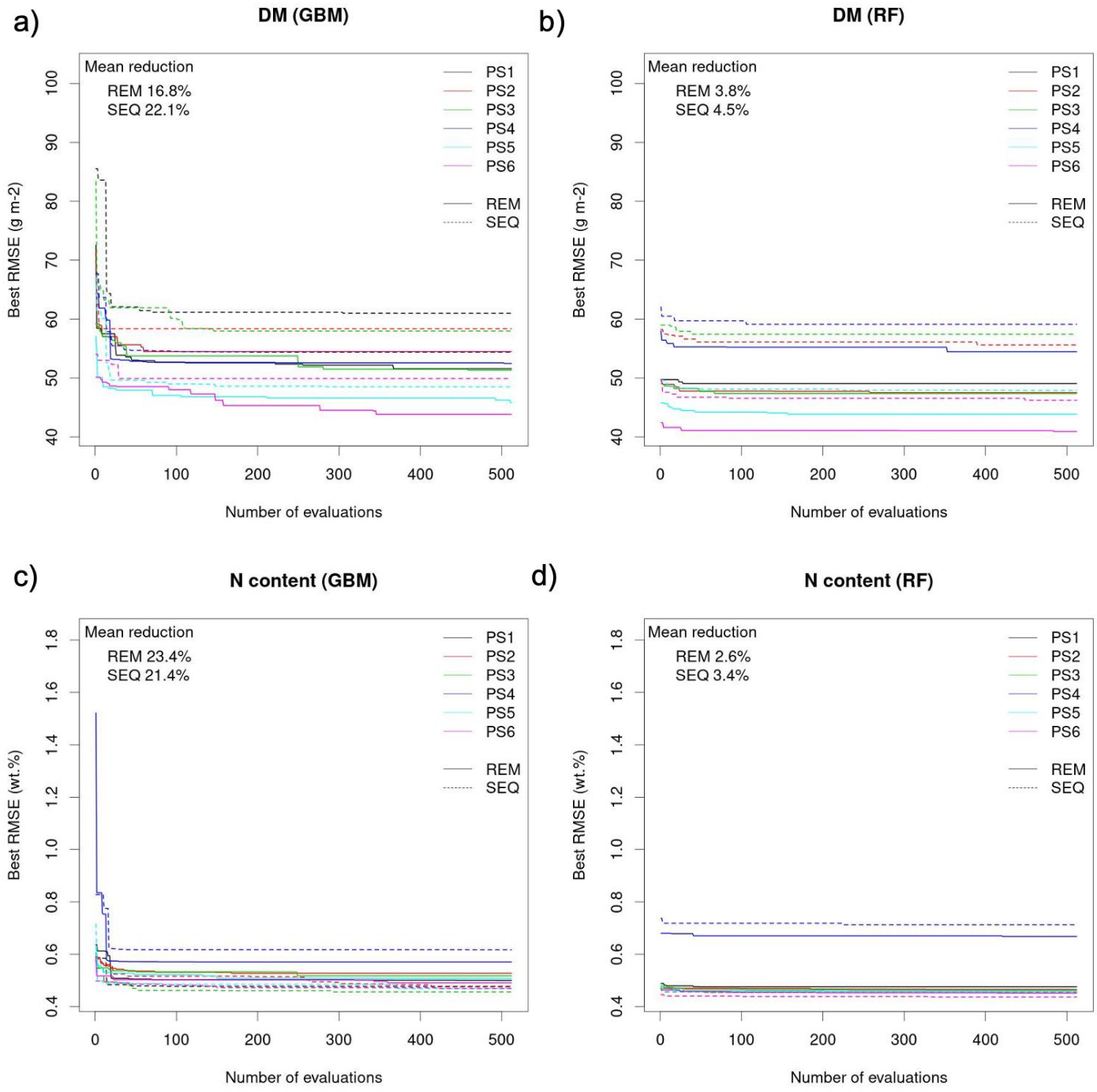

Figure SF2. Changes of best error (i.e. lowest error achieved until i_{th} iteration) in parameter calibration for a) DM with GBM, b) DM with RF, c) N concentration with GBM, d) N concentration with RF algorithm. The overall improvement (i.e. mean of mean reductions) is 11.0%. Note that initial model performance is based on 12 randomly sampled parameter values from the given ranges.

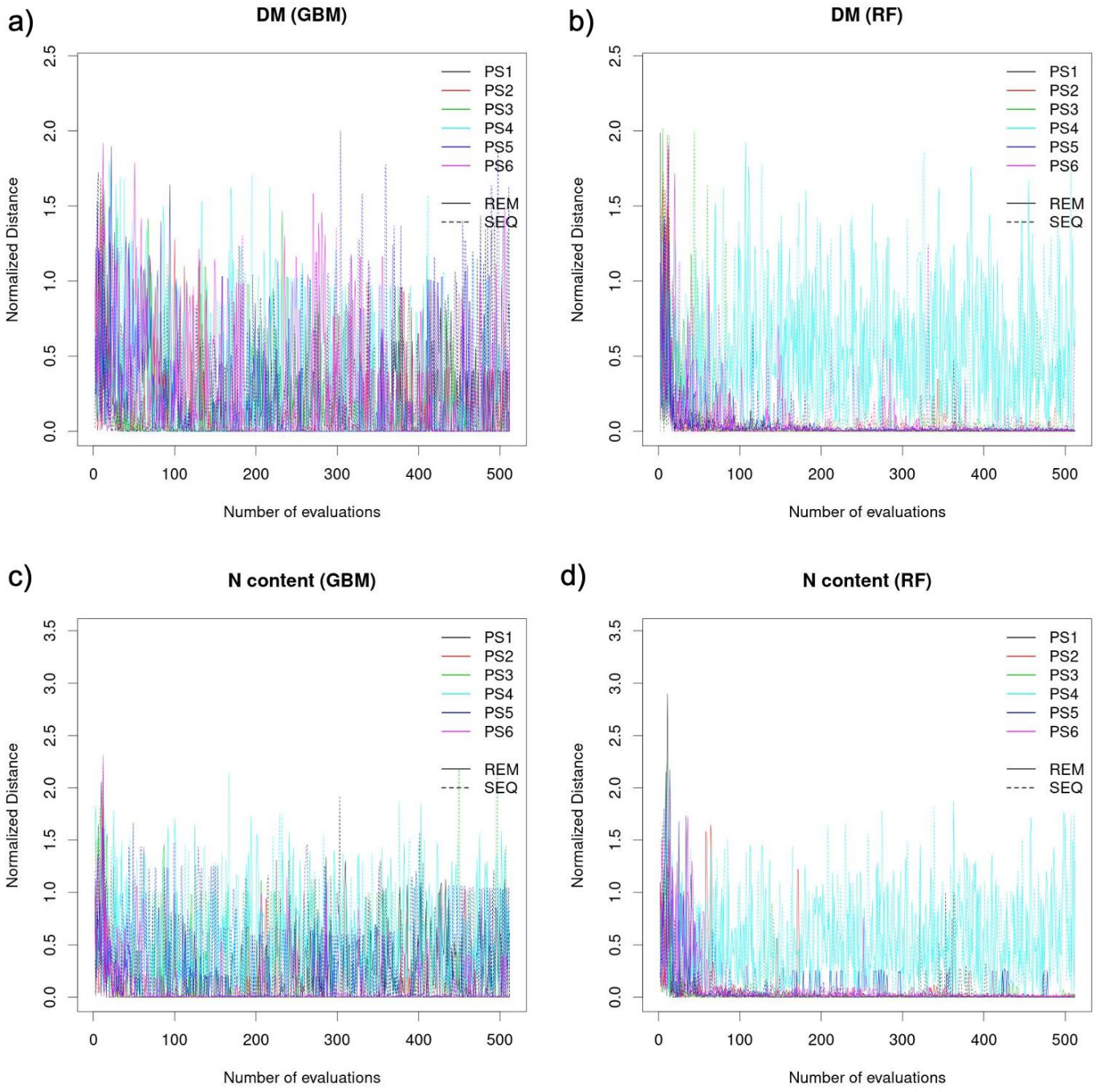

Figure SF3. Parameter convergence diagnosis by normalized distance for a) DM with GBM, b) DM with RF, c) N concentration with GBM, d) N concentration with RF algorithm. The metric is defined by distance between two consecutive parameter proposals after normalization quantifying how similar proposals are at each time step. Note that initial model performance is based on 12 randomly sampled parameter values from the given ranges.

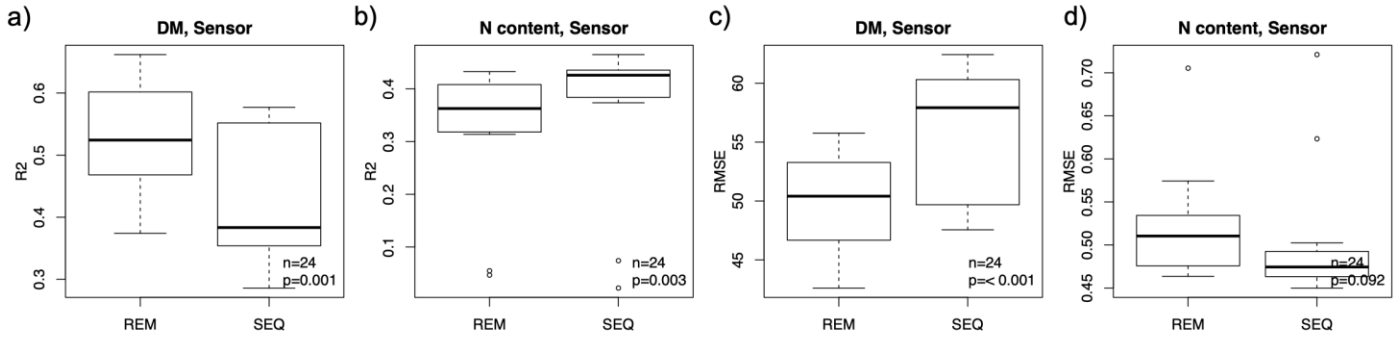

Figure SF4. Comparison of model quality parameters between REM and SEQ data: a) R^2 of DM models, b) R^2 of N concentration models, c) RMSE of DM models, d) RMSE of N concentration models. The boxplots were calculated from the model performance metrics of all ML algorithm and predictor set combinations of the respective sensor. The p-values are from Wilcoxon signed rank test for paired samples.

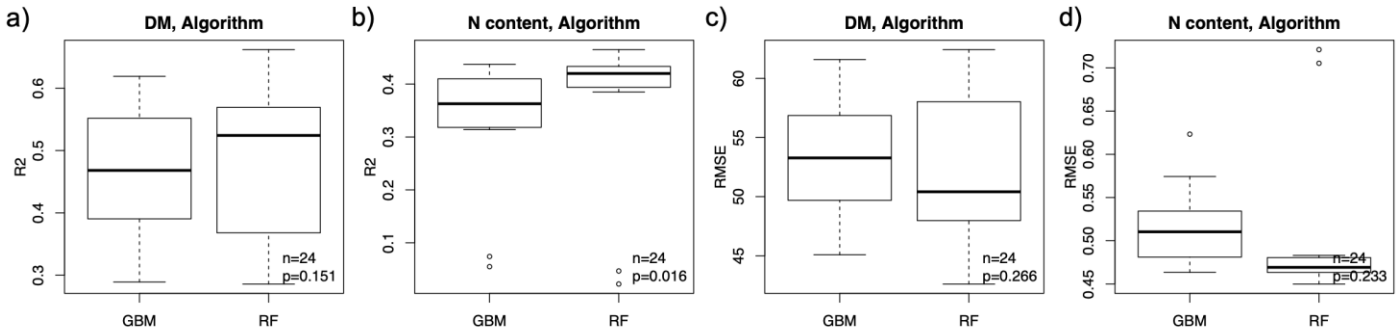

Figure SF5. Comparison of model quality parameters between the ML algorithms GBM and RF: a) R^2 of DM models, b) R^2 of N concentration models, c) RMSE of DM models, d) RMSE of N concentration models. The boxplots were calculated from the model performance metrics of all sensor and predictor set combinations of the respective ML algorithm. The p-values are from Wilcoxon signed rank test for paired samples.

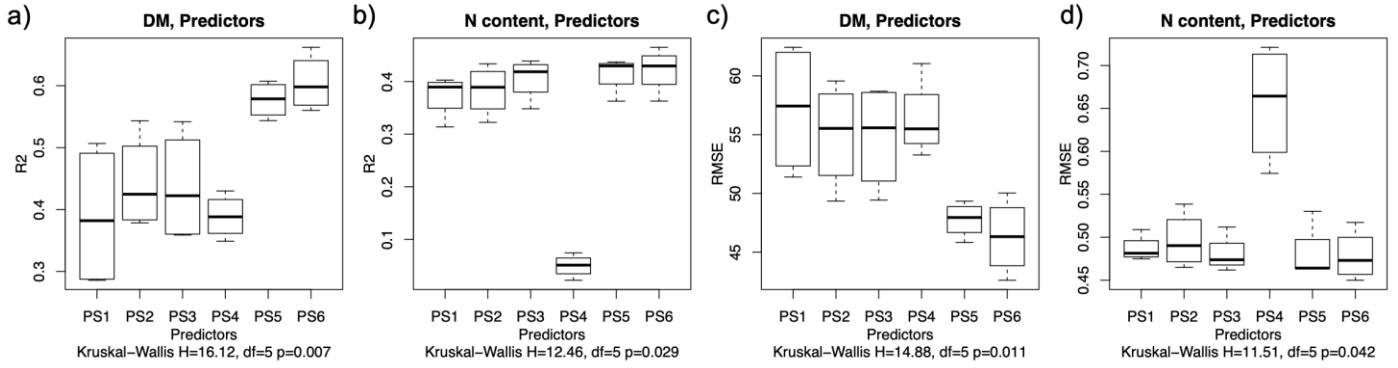

Figure SF6. Comparison of model quality parameters between different predictor sets: a) R^2 of DM models, b) R^2 of N concentration models, c) RMSE of DM models, d) RMSE of N concentration models. The boxplots were calculated from the model performance metrics of all sensor and ML algorithm combinations of the respective predictor set. The p-values are from Kruskal-Wallis rank sum. Predictor sets PS1: raw reflectance data; PS2: raw reflectance data + canopy height; PS3: raw reflectance data + VI; PS4: raw reflectance data + VI + canopy height; PS5: canopy height; PS6: VI) test.

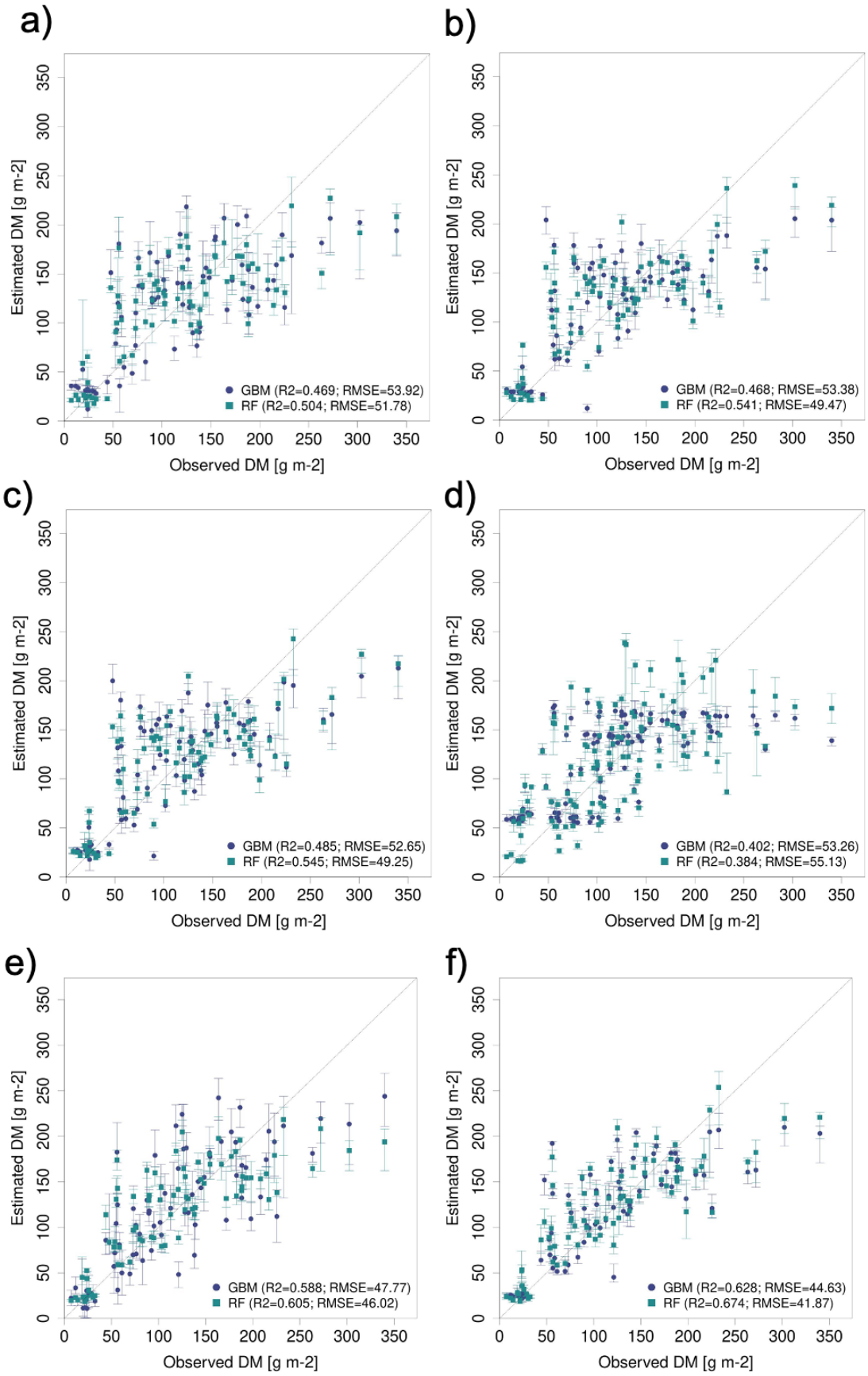

Figure SF7-1. Prediction plots of DM for cross-validation sites (FE + RB) with REM data: a) for predictor set PS1 (raw reflectance data), b) for PS2 (VI), c) for PS3 (raw reflectance data + VI), d) for PS4 (canopy height), e) for PS5 (raw reflectance data + canopy height), f) for PS6 (raw reflectance data + VI + canopy height). The error bars reflect 90% prediction intervals, defined by 5th and 95th percentiles of the 10 iterations.

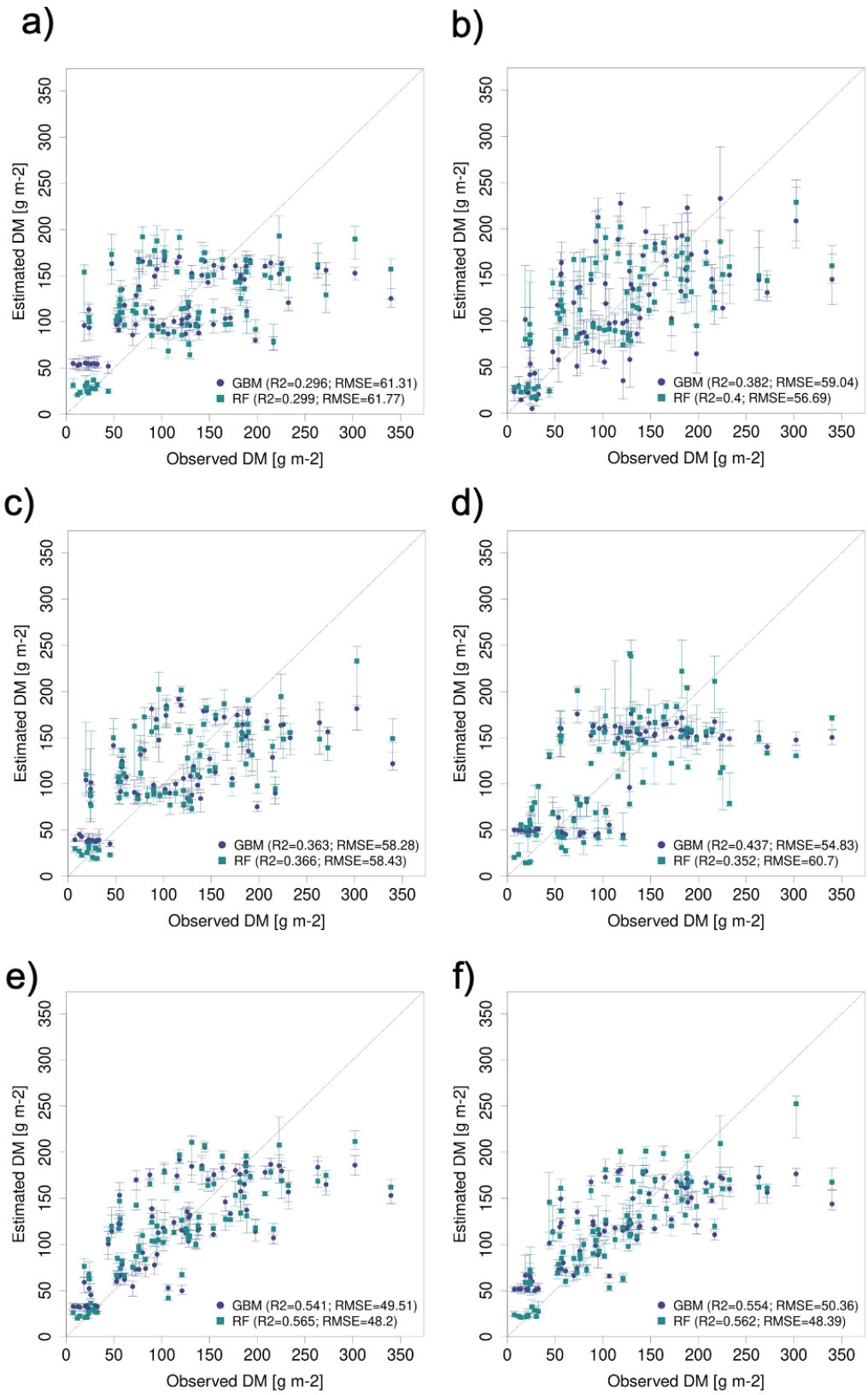

Fig. SF7-2 Prediction plots of DM for cross-validation sites (FE + RB) with SEQ data: a) for predictor set PS1 (raw reflectance data), b) for PS2 (VI), c) for PS3 (raw reflectance data + VI), d) for PS4 (canopy height), e) for PS5 (raw reflectance data + canopy height), f) for PS6 (raw reflectance data + VI + canopy height). The error bars reflect 90% prediction intervals, defined by 5th and 95th percentiles of the 10 iterations.

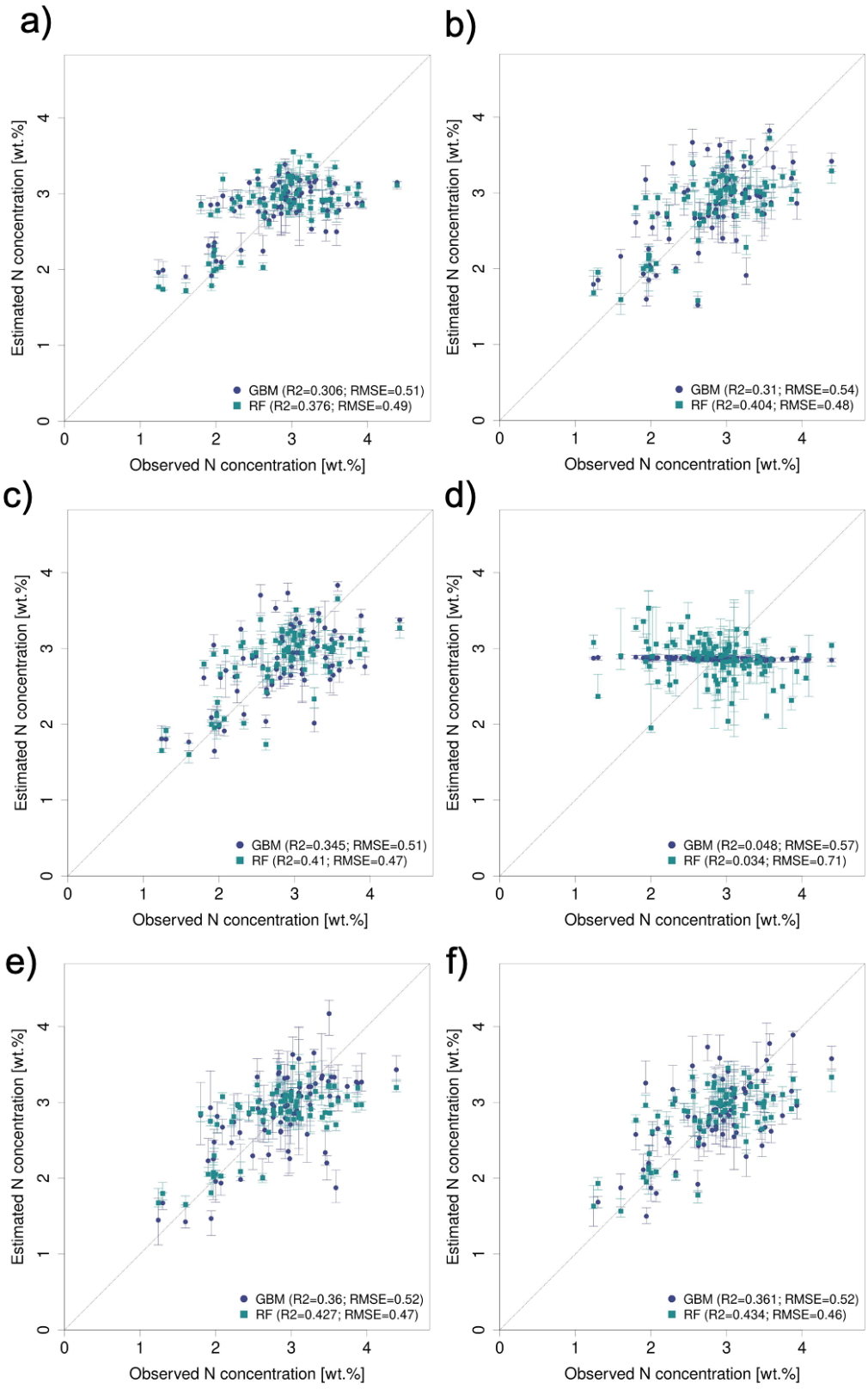

Figure SF8-1. Prediction plots of N concentration for cross-validation sites (FE + RB) with REM data: a) for predictor set PS1 (raw reflectance data), b) for PS2 (VI), c) for PS3 (raw reflectance data + VI), d) for PS4 (canopy height), e) for PS5 (raw reflectance data + canopy height), f) for PS6 (raw reflectance data + VI + canopy height). The error bars reflect 90% prediction intervals, defined by 5th and 95th percentiles of the 10 iterations.

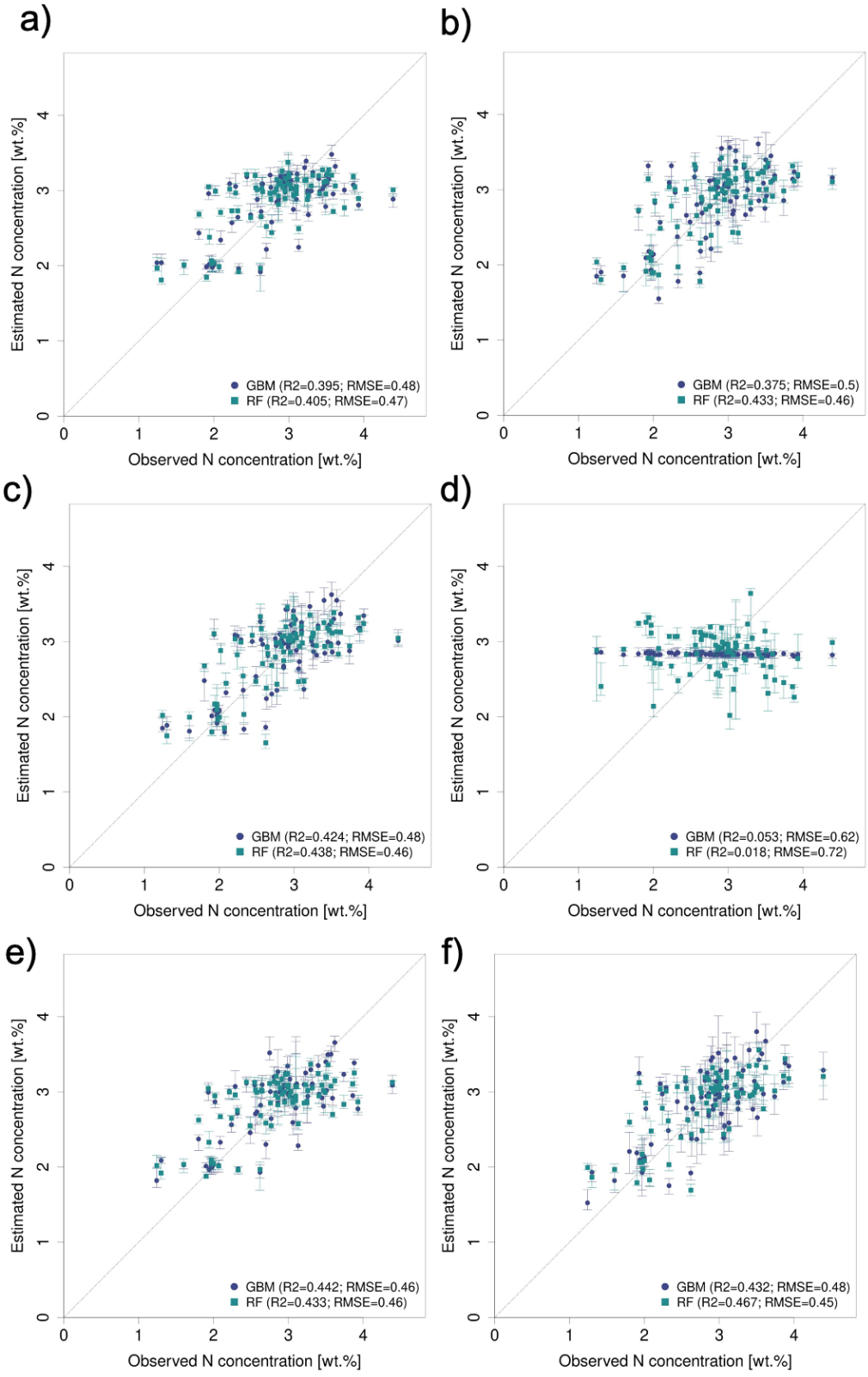

Fig SF8-2. Prediction plots of N concentration for cross-validation sites (FE + RB) with SEQ data: a) for predictor set PS1 (raw reflectance data), b) for PS2 (VI), c) for PS3 (raw reflectance data + VI), d) for PS4 (canopy height), e) for PS5 (raw reflectance data + canopy height), f) for PS6 (raw reflectance data + VI + canopy height). The error bars reflect 90% prediction intervals, defined by 5th and 95th percentiles of the 10 iterations.

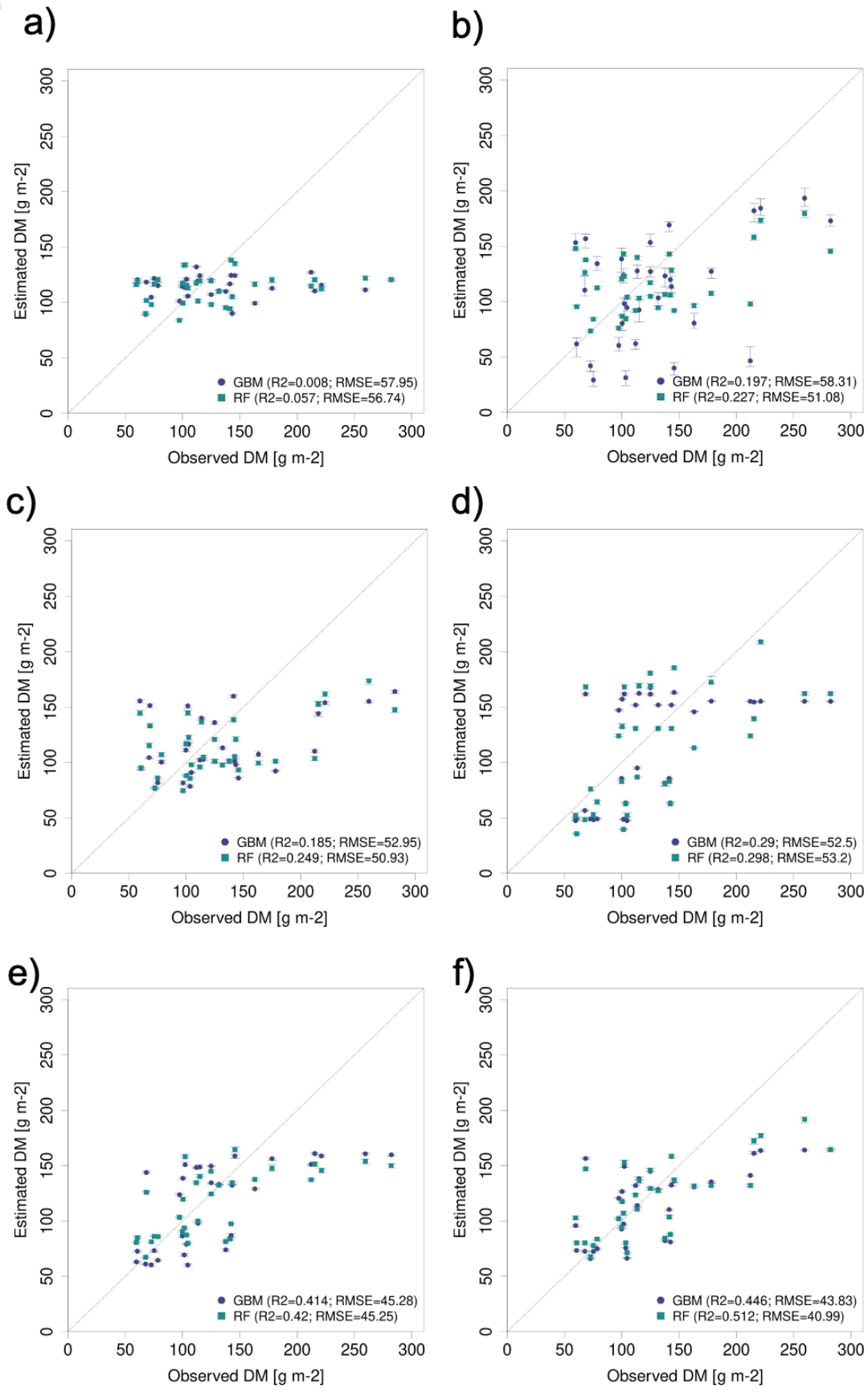

Figure SF9. Prediction plots of DM for validation site (EL) with SEQ data: a) for predictor set PS1 (raw reflectance data), b) for PS2 (VI), c) for PS3 (raw reflectance data + VI), d) for PS4 (canopy height), e) for PS5 (raw reflectance data + canopy height), f) for PS6 (raw reflectance data + VI + canopy height). The error bars reflect 90% prediction intervals, defined by 5th and 95th percentiles of the 10 iterations.

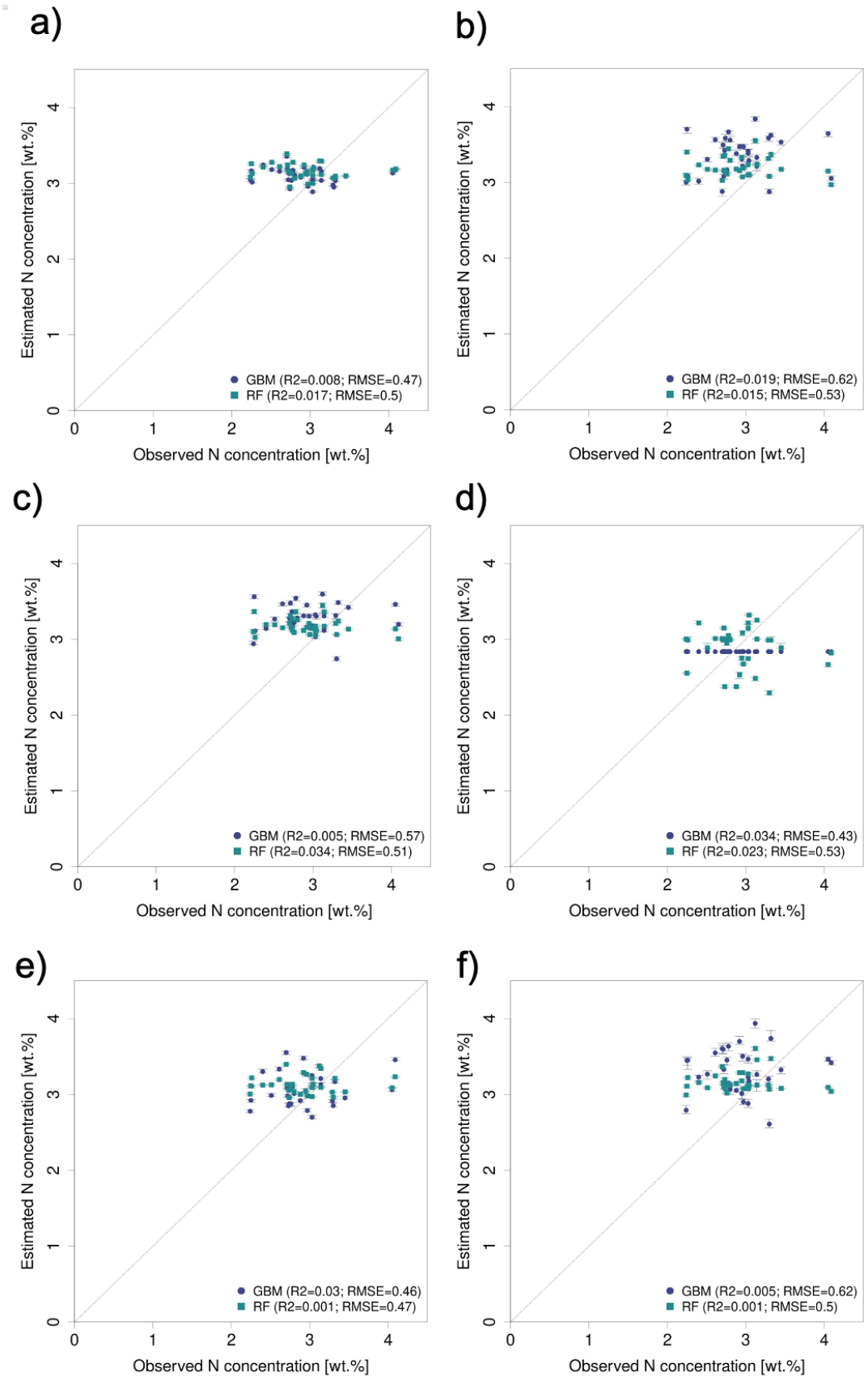

Figure SF10. Prediction plots of N concentration for validation site (EL) with SEQ data: a) for predictor set PS1 (raw reflectance data), b) for PS2 (VI), c) for PS3 (raw reflectance data + VI), d) for PS4 (canopy height), e) for PS5 (raw reflectance data + canopy height), f) for PS6 (raw reflectance data + VI + canopy height). The error bars reflect 90% prediction intervals, defined by 5th and 95th percentiles of the 10 iterations.

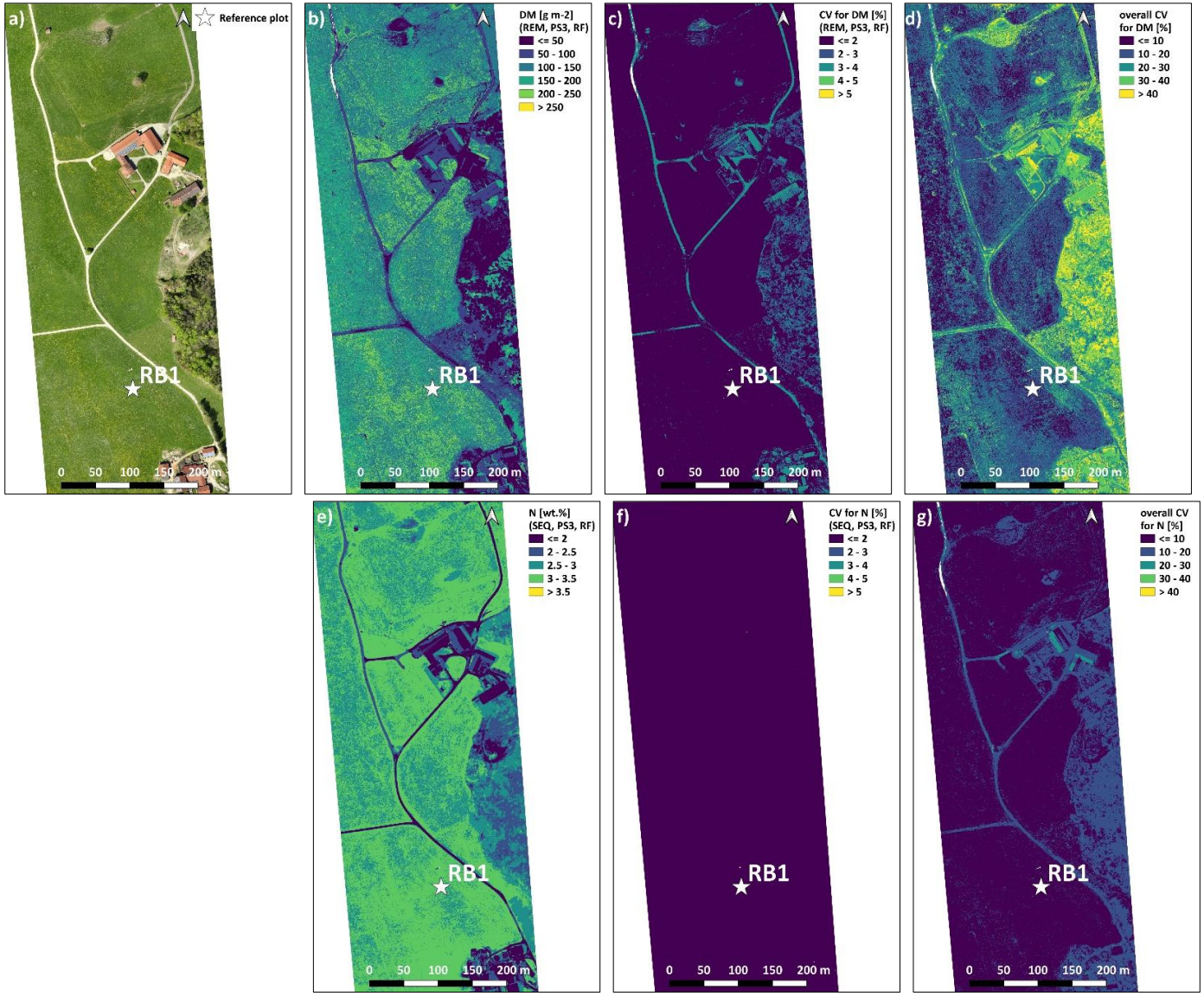

Figure SF11. Spatial estimations for RB-South site. a) Orthophoto for comparison, b) DM with an REM-PS3-RF combination, c) CV of DM with an REM-PS3-RF combination, d) Overall CV of DM for all PS1, PS2 and PS3 models, e) N concentration with an SEQ-PS3-RF combination, b) CV of N concentration with SEQ-PS3-RF combination, c) Overall CV of N concentration for all PS1, PS2 and PS3 models. Estimation of DM and N concentration represents the mean of the 10 iterations for the selected model. Note that spatial estimates are only valid for pixels of unshaded and vegetated grassland.

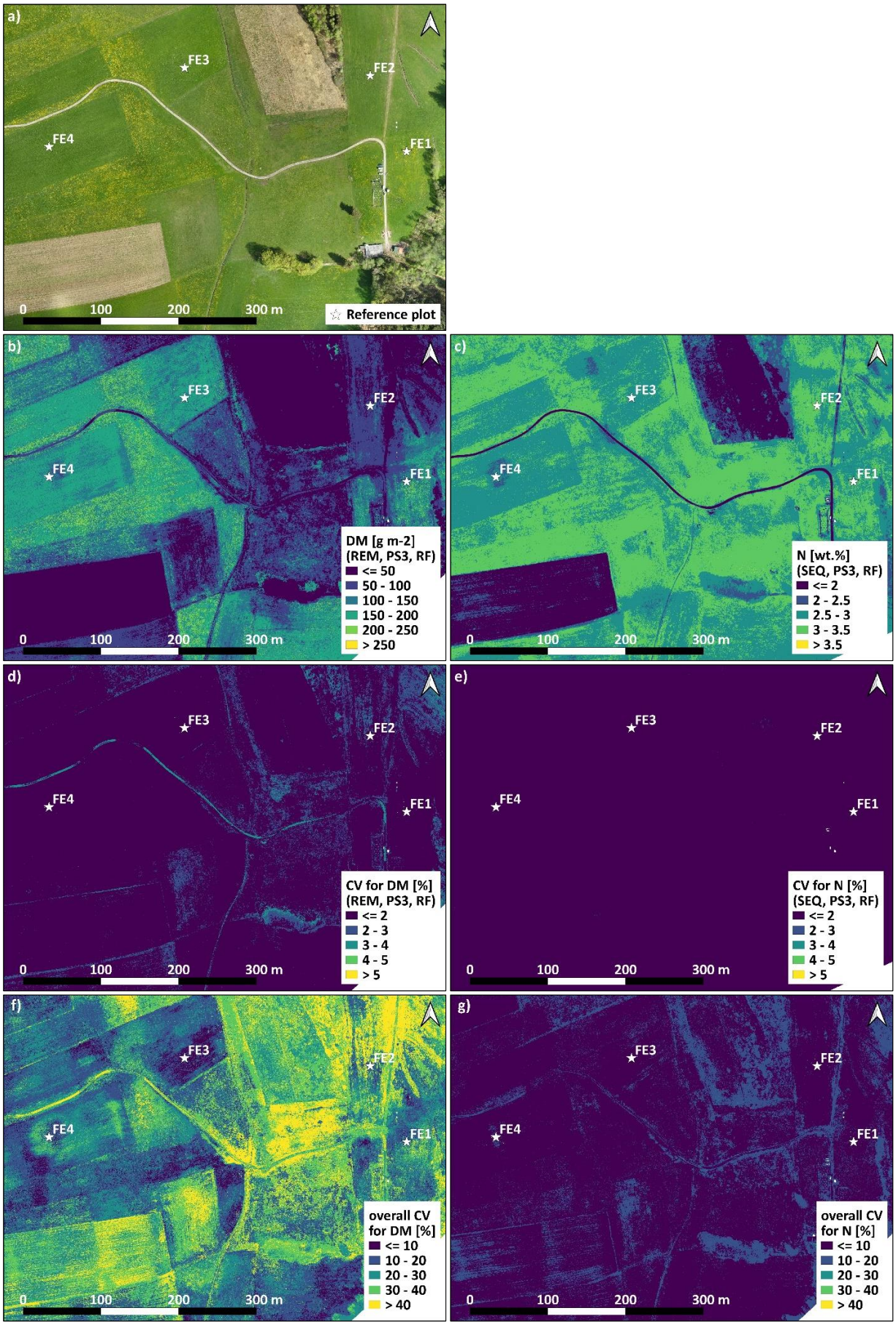

Figure SF12. Spatial estimations for FE site. a) Orthophoto for comparison, b) DM with an REM-PS3-RF combination, c) N concentration with an SEQ-PS3-RF combination, d) CV of DM with an REM-PS3-RF combination, e) CV of N concentration with an SEQ-PS3-RF combination, f) Overall CV of DM for all PS1, PS2 and PS3 models, g) Overall CV of N concentration for all PS1, PS2 and PS3 models. Estimation of DM and N concentration represents the mean of the 10 iterations for the selected model. Note that spatial estimates are only valid for pixels of unshaded and vegetated grassland.

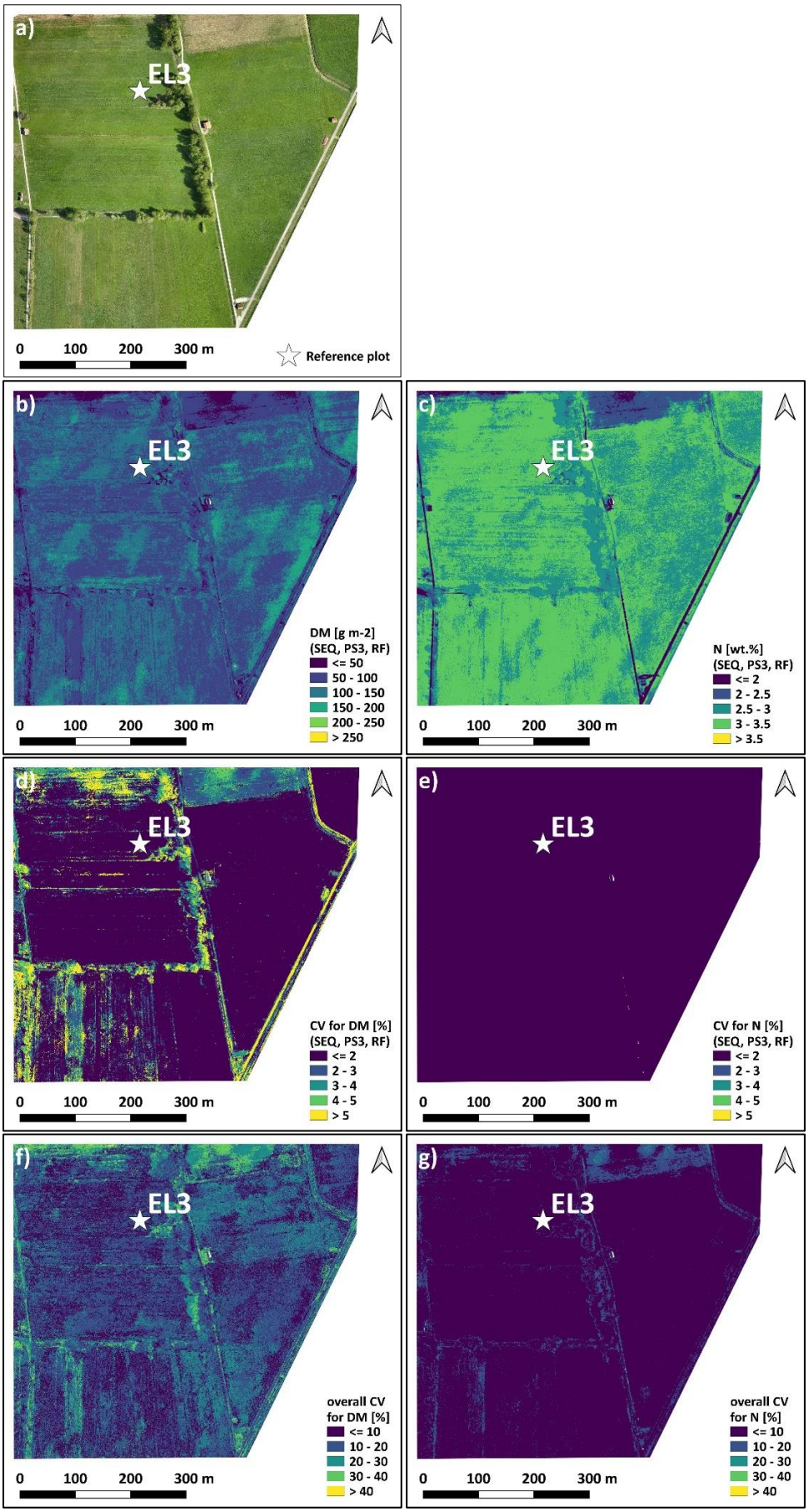

Figure SF13. Spatial estimations for EL-North site. a) Orthophoto for comparison, b) DM with an SEQ-PS3-RF combination, c) N concentration with an SEQ-PS3-RF combination, d) CV of DM with an SEQ-PS3-RF combination, e) CV of N concentration with an SEQ-PS3-RF combination, f) Overall CV of DM for all PS1, PS2 and PS3 models, g) Overall CV of N concentration for all PS1, PS2 and PS3 models. Estimation of DM and N concentration represents the mean of the 10 iterations for the selected model. Note that spatial estimates are only valid for pixels of unshaded and vegetated grassland.

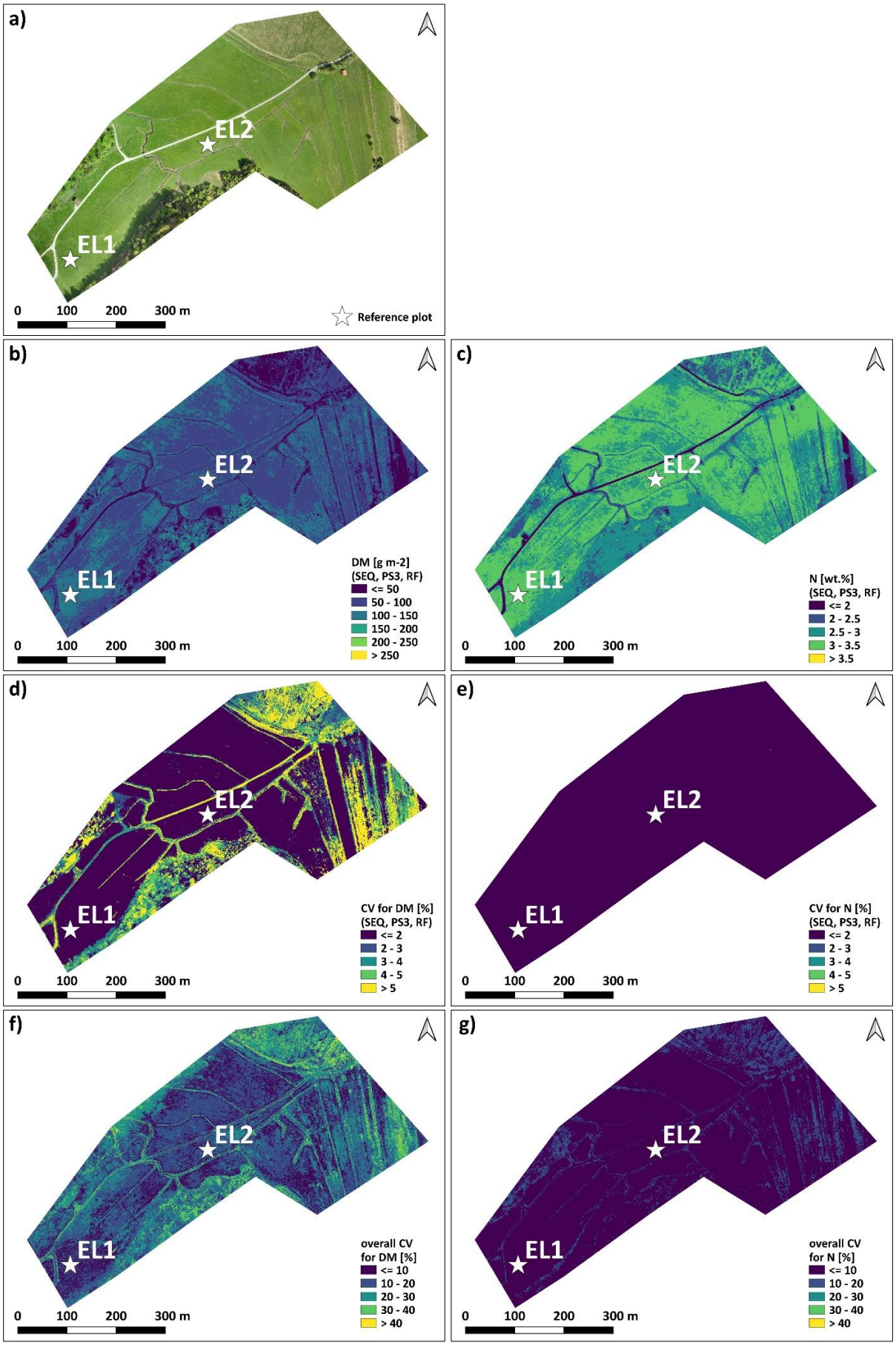

Figure SF14. Spatial estimations for EL-South site. a) Orthophoto for comparison, b) DM with an SEQ-PS3-RF combination, c) N concentration with an SEQ-PS3-RF combination, d) CV of DM with an SEQ-PS3-RF combination, e) CV of N concentration with an SEQ-PS3-RF combination, f) Overall CV of DM for all PS1, PS2 and PS3 models, g) Overall CV of N concentration for all PS1, PS2 and PS3 models. Estimation of DM and N concentration represents the mean of the 10 iterations for the selected model. Note that spatial estimates are only valid for pixels of unshaded and vegetated grassland.

References of supplementary material

Asam, S.: Potential of high resolution remote sensing data for Leaf Area Index derivation using statistical and physical models, PhD thesis, Julius-Maximilians-University Würzburg, Würzburg, 228 pp., 2014.

Blackburn, G. A.: Quantifying chlorophylls and caroteniods at leaf and canopy scales: An evaluation of some hyperspectral approaches, Remote Sens. Environ., 66, 273–285, https://doi.org/10.1016/S0034-4257(98)00059-5, 1998.

Blackburn, G. A.: Relationships between spectral reflectance and pigment concentrations in stacks of deciduous broadleaves, Remote Sens. Environ., 70, 224–237, https://doi.org/10.1016/S0034-4257(99)00048-6, 1999.

Broge, N. H. and Leblanc, E.: Comparing prediction power and stability of broadband and hyperspectral vegetation indices for estimation of green leaf area index and canopy chlorophyll density, Remote Sens. Environ, 76, 156–172, https://doi.org/10.1016/S0034-4257(00)00197-8, 2001.

Chappelle, E. W., Kim, M. S., and McMurtrey, J. E.: Ratio analysis of reflectance spectra (RARS): An algorithm for the remote estimation of the concentrations of chlorophyll A, chlorophyll B, and carotenoids in soybean leaves, Remote Sens. Environ, 39, 239–247, https://doi.org/10.1016/0034-4257(92)90089-3, 1992.

Chen, J. M.: Evaluation of vegetation indices and a modified simple ratio for Boreal applications, Can. J. Remote Sens., 22, 229–242, https://doi.org/10.1080/07038992.1996.10855178, 1996.

Datt, B.: Visible/near infrared reflectance and chlorophyll concentration in Eucalyptus leaves, Int. J. Remote Sens., 20, 2741–2759, https://doi.org/10.1080/014311699211778, 1999.

Daughtry, C. S. , Walthall, C., Kim, M., de Colstoun, E. B., and McMurtrey, J.: Estimating corn leaf chlorophyll concentration from leaf and canopy reflectance, Remote Sens. Environ., 74, 229–239, https://doi.org/10.1016/S0034-4257(00)00113-9, 2000.

Ehammer, A., Fritsch, S., Conrad, C., Lamers, J., and Dech, S.: Statistical derivation of fPAR and LAI for irrigated cotton and rice in arid Uzbekistan by combining multi-temporal RapidEye data and ground measurements, Proc.SPIE, https://doi.org/10.1117/12.864796, 2010.

Gitelson, A. and Merzlyak, M. N.: Spectral reflectance changes associated with autumn senescence of Aesculus hippocastanum L. and Acer platanoides L. leaves. Spectral features and relation to chlorophyll estimation, J. Plant Physiol., 143, 286–292, https://doi.org/10.1016/S0176-1617(11)81633-0, 1994.

Gitelson, A. A. and Merzlyak, M. N.: Remote estimation of chlorophyll concentration in higher plant leaves, Int. J. Remote Sens., 18, 2691–2697, https://doi.org/10.1080/014311697217558, 1997.

Haboudane, D., Miller, J. R., Pattey, E., Zarco-Tejada, P. J., and Strachan, I. B.: Hyperspectral vegetation indices and novel algorithms for predicting green LAI of crop canopies: Modeling and validation in the context of precision agriculture, Remote Sens. Environ., 90, 337–352, https://doi.org/10.1016/j.rse.2003.12.013, 2004.

Huete, A., Didan, K., Miura, T., Rodriguez, E., Gao, X., and Ferreira, L.: Overview of the radiometric and biophysical performance of the MODIS vegetation indices, Remote Sens. Environ., 83, 195–213, https://doi.org/10.1016/S0034-4257(02)00096-2, 2002.

Huete, A. R.: A soil-adjusted vegetation index (SAVI), Remote Sens. Environ., 25, 295–309, https://doi.org/10.1016/0034-4257(88)90106-X, 1988.

Jordan, C. F.: Derivation of leaf-area index from quality of light on the forest floor, Ecology, 50, 663–666, 1969.

Kaufman, Y. J. and Tanre, D.: Atmospherically resistant vegetation index (ARVI) for EOS-MODIS, IEEE T. Geosci. Remote, 30, 261–270, https://doi.org/10.1109/36.134076, 1992.

Ollinger, S. V.: Sources of variability in canopy reflectance and the convergent properties of plants, New Phytol., 189, 375–394, https://doi.org/10.1111/j.1469-8137.2010.03536.x, 2011.

Pearson, R. L., Miller, L. D.: Remote mapping of standing crop biomass for estimation of the productivity of the shortgrass prairie, Pawnee National Grasslands, Colorado, in: Proceedings of the Eighth International Symposium on Remote Sensing of Environment Dept., Fort Collins, Colorado, 1357-1381, 1972.

Penuelas, J., Baret, F., and Filella, I.: Semi-Empirical Indices to Assess Carotenoids/Chlorophyll-a Ratio from Leaf Spectral Reflectance, Photosynthetica, 32, 221–230, 1995.

Qi, J., Chehbouni, A., Huete, A. R., Kerr, Y. H., and Sorooshian, S.: A modified soil adjusted vegetation index, Remote Sens. Environ., 48, 119–126, https://doi.org/10.1016/0034-4257(94)90134-1, 1994.

Rondeaux, G., Steven, M., and Baret, F.: Optimization of soil-adjusted vegetation indices, Remote Sens. Environ., 55, 95–107, https://doi.org/10.1016/0034-4257(95)00186-7, 1996.

Roujean, J.-L. and Breon, F.-M.: Estimating PAR absorbed by vegetation from bidirectional reflectance measurements, Remote Sens. Environ., 51, 375–384, https://doi.org/10.1016/0034-4257(94)00114-3, 1995.

Rouse, J., Haas, R., Schell, J., and Deering, J.: Monitoring vegetation systems in the Great Plains with ERTS, in: NASA SP- 351: Proceedings of the Third Symposium on Significant Results Obtained with ERTS-1, Third Symposium on Significant Results Obtained with ERTS-1, Washington , D.C., 309–317, 1974.

Sims, D. A. and Gamon, J. A.: Relationships between leaf pigment concentration and spectral reflectance across a wide range of species, leaf structures and developmental stages, Remote Sens. Environ., 81, 337–354, https://doi.org/10.1016/S0034-4257(02)00010-X, 2002.